NASA/TM—2002-211906/PART1

A Deterministic Interfacial Cyclic Oxidation Spalling Model: Part 1.—Model Development and Parametric Response

James L. Smialek
Glenn Research Center, Cleveland, Ohio

December 2002

The NASA STI Program Office . . . in Profile

Since its founding, NASA has been dedicated to the advancement of aeronautics and space science. The NASA Scientific and Technical Information (STI) Program Office plays a key part in helping NASA maintain this important role.

The NASA STI Program Office is operated by Langley Research Center, the Lead Center for NASA's scientific and technical information. The NASA STI Program Office provides access to the NASA STI Database, the largest collection of aeronautical and space science STI in the world. The Program Office is also NASA's institutional mechanism for disseminating the results of its research and development activities. These results are published by NASA in the NASA STI Report Series, which includes the following report types:

- TECHNICAL PUBLICATION. Reports of completed research or a major significant phase of research that present the results of NASA programs and include extensive data or theoretical analysis. Includes compilations of significant scientific and technical data and information deemed to be of continuing reference value. NASA's counterpart of peer-reviewed formal professional papers but has less stringent limitations on manuscript length and extent of graphic presentations.

- TECHNICAL MEMORANDUM. Scientific and technical findings that are preliminary or of specialized interest, e.g., quick release reports, working papers, and bibliographies that contain minimal annotation. Does not contain extensive analysis.

- CONTRACTOR REPORT. Scientific and technical findings by NASA-sponsored contractors and grantees.

- CONFERENCE PUBLICATION. Collected papers from scientific and technical conferences, symposia, seminars, or other meetings sponsored or cosponsored by NASA.

- SPECIAL PUBLICATION. Scientific, technical, or historical information from NASA programs, projects, and missions, often concerned with subjects having substantial public interest.

- TECHNICAL TRANSLATION. English-language translations of foreign scientific and technical material pertinent to NASA's mission.

Specialized services that complement the STI Program Office's diverse offerings include creating custom thesauri, building customized databases, organizing and publishing research results . . . even providing videos.

For more information about the NASA STI Program Office, see the following:

- Access the NASA STI Program Home Page at ***http://www.sti.nasa.gov***

- E-mail your question via the Internet to help@sti.nasa.gov

- Fax your question to the NASA Access Help Desk at 301–621–0134

- Telephone the NASA Access Help Desk at 301–621–0390

- Write to:
  NASA Access Help Desk
  NASA Center for AeroSpace Information
  7121 Standard Drive
  Hanover, MD 21076

NASA/TM—2002-211906/PART1

A Deterministic Interfacial Cyclic Oxidation Spalling Model: Part 1.—Model Development and Parametric Response

James L. Smialek
Glenn Research Center, Cleveland, Ohio

National Aeronautics and
Space Administration

Glenn Research Center

December 2002

Acknowledgments

The many cyclic oxidation model data sets were only made possible by a customized, user-friendly, computer program designed by Dr. Judith V. Auping as an adjunct model to our COSP for Windows®, product. For this effort I am truly grateful.

This report is a formal draft or working paper, intended to solicit comments and ideas from a technical peer group.

This report contains preliminary findings, subject to revision as analysis proceeds.

Available from

NASA Center for Aerospace Information
7121 Standard Drive
Hanover, MD 21076

National Technical Information Service
5285 Port Royal Road
Springfield, VA 22100

Available electronically at http://gltrs.grc.nasa.gov

A Deterministic Interfacial Cyclic Oxidation Spalling Model: Part 1.—Model Development and Parametric Response

James L. Smialek
National Aeronautics and Space Administration
Glenn Research Center
21000 Brookpark Road
Cleveland, Ohio 44135

Abstract.—An equation has been developed to model the iterative scale growth and spalling process that occurs during cyclic oxidation of high temperature materials. Parabolic scale growth and spalling of a constant surface area fraction have been assumed. Also, interfacial spallation of the only the thickest segments was assumed. This simplicity allowed for representation by a simple deterministic summation series. Inputs are the parabolic growth rate constant, the spall area fraction, oxide stoichiometry, and cycle duration. Outputs include the net weight change behavior, as well as the total amount of oxygen and metal consumed, the total amount of oxide spalled, and the mass fraction of oxide spalled. The outputs all follow typical well-behaved trends with the inputs and are in good agreement with previous interfacial models.

1. Introduction

Oxidation is a process important to any high temperature metal component operating in air or oxygen. For isothermal exposures, the rate of oxidation determines the rate of material consumption. Both are generally controlled by solid state diffusion through the scale layer and show approximately parabolic kinetics in which the instantaneous rate is inversely proportional to the existing scale thickness. Many components, however, experience cyclic oxidation in applications that entail periodic start-up and shutdown. Typically, some scale spallation may occur upon cooling, resulting in loss of the protective diffusion barrier provided by a fully intact scale. Upon reheating, the component will therefore experience accelerated oxidation in the spalled regions because of the inverse rate dependence upon thickness.

Cyclic oxidation testing has therefore been a mainstay of material characterization and performance ranking for high temperature materials. The engineering response is generally characterized nondestructively by weight change curves and surface recession. Scanning and optical microscopy of scale morphology, phase identification by x-ray diffraction, and electron probe analyses of alloy depletion zones all help characterize the mechanisms of degradation. A general trend of surface recession follows an empirical cyclic oxidation weight change 'attack parameter', which takes into account degradation by both scale growth and spallation [1]. However, a direct quantitative relationship between cyclic weight change and material degradation (i.e., metal consumed) is not normally measured.

One important step toward approaching this direct relationship has been the development of mathematical cyclic oxidation spalling models which attempt to represent the discreet processes that occur each time the scale spalls upon cooling and re-grows upon heating. In general, a scale growth law is postulated with a set rate constant, and a spalling formalism is defined which dictates the type and amount of spalling that occurs each cycle. This unit process is formally described by means of an algorithm, by which an iterative calculation may generate the entire cyclic oxidation curve. This has been done for the case of interfacial spalling, where a constant area fraction of each portion of the scale has been proposed to spall each cycle [2].

It has also been done for the case where a uniform external layer of specified thickness spalls off the entire area. Here the fractional thickness that spalls is a direct function of the existing scale thickness [3]. This spalling criterion has been further modified to allow for non-uniform or bimodal spallation, in which some segments do not spall at all on a given cycle, while others spall some fixed ratio of the thickness - including the possibility of total interfacial spallation [4]. This generalized model allows for the selection of various scale growth laws, various spalling dependency rules, and either uniform or bimodal spalling geometry. (Publicly available for DOS and Windows 95, 98, and 2000 operating systems) [4,5].

It is useful to describe experimental cyclic oxidation behavior in terms of these models after a reasonable fit has been obtained by adjustments of the various input parameters. The basic strategy has been to specify a scale phase and k_p known or measured for the alloy, then find the best fit by adjusting the spalling model parameters [5]. The growth rate could also be approximated from fitting the early portion of a typical cyclic oxidation curve, during which time very little spallation effects are evident.

The ultimate utility of such fitted models is the ability to predict very long-term behavior from less time-consuming, short-term tests, assuming that no mechanistic changes take place. Another value to the models is the ability to extract the amount of metal consumed as one of the calculated outputs. This is the most direct figure of merit regarding material degradation. When a cyclic oxidation model is coupled with a diffusion model of selective oxidation, the prediction of solute depletion and the transition to non-protective oxidation behavior is enabled for coatings and alloys [6]. (Many related contributions have been presented in a recent summary paper [7], along with many pertinent high temperature cyclic oxidation topics [8]).

Families of model curves exhibit consistent regularity and trends in reference to the input parameters (growth rate, spalling constant, oxide phase, and cycle duration). The characteristic features of the weight change curve (maximum weight, cycles to maximum, cycles to zero weight change, and terminal rate of weight loss) have thus been described in terms of these inputs [2,4,5,7], as discovered by trial functions and regression analyses. However, precise mathematical dependencies have eluded derivation. Indeed, the model cyclic weight change curve itself cannot be obtained analytically, but relies totally upon series summations or iterative calculations.

Independent measurements of the growth rate have generally agreed with the growth rates obtained from model fits to cyclic data. However there is little independent

verification or prediction of the amount of scale that should spall each cycle. At best, it has been observed experimentally that the amount of spalling, on either absolute or relative terms, increases with scale thickness. These conclusions were made by both weight change and surface area measurements [2,3]. However, the actual distribution of thickness and lateral dimensions (area) of the spalled segments is much more difficult to obtain.

Ideally, a mechanical model would address the critical stress in the scale and the type and degree of spallation that occurs each cycle. Substantial progress toward understanding the fracture mechanics and spallation of scales has been made. In general, oxide scales have lower coefficients of thermal expansion than their metal substrates and are subjected to large compressive stresses upon cooling. This stress is commonly accepted as the primary cause of spallation and is additive to any growth stresses that are retained after cooldown. The description of scale spallation as a buckling instability of the scale or as wedge-driven crack growth has been presented in an extensive review [9]. The growth and thermal stresses generated in protective alumina scales have been elegantly and thoroughly studied through the use of photo-stimulated luminescence (piezospectroscopy) [10]. Furthermore , the size of a spall segment has been modeled from the strain energy in the scale, the scale thickness, and interfacial toughness. [11,12]. These studies are leading the way to postulate the morphology and quantity of spalling.

Ultimately, the relationship between cyclic weight change (scale spallation) and mechanics-based approaches may be drawn. Indeed, other studies have modeled the cyclic weight change curve with fracture mechanics-based models by using adjustable parameters based on the scale (or interface) fracture toughness [13] or stored strain energy [14]. Both approaches met with good success, although these fitted parameters were not independently generated. Therefore, at the present time, empirical fitting remains the primary means by which a cyclic oxidation weight change curve is modeled.

The purpose of the present paper is to present the development of a simple model simulation that assumes interfacial spallation to the bare metal surface every cycle. Furthermore, this spallation is biased toward the thickest oxide regions that have yet to spall, as would be suggested by the previous analyses [2-14]. One or both of these features has been observed on commercial NiAl and occasionally Ni(Pt)Al bond coatings, as well as on uncoated single crystal superalloys [15,16,17]. The model simplicity propagates into the mathematical formulations, such that a more direct relationship between the input parameters (stoichiometry, atomic weight, growth rate, cycle duration, and spall area fraction) and the cyclic oxidation response (weight change, amount spalled, amount of metal consumed) can be easily discerned. In Part 2, all the features of the cyclic oxidation curve are described by simple algebraic functions. This new perspective leads to some generalization of all possible combinations of the input parameters and to the development of a universal, normalized cyclic oxidation curve.

2. Model Development

2.1 Weight change equations.

According to the most basic diffusional models of oxidation, a scale will grow with parabolic kinetics, such that the sample weight (mass) gain per unit area, $\Delta W/A$, is given by

$$\Delta W / A = \sqrt{k_p \Delta t} \ , \qquad [1]$$

for a parabolic oxidation rate constant of k_p and heating cycle time of Δt, (see Appendix for a glossary of symbols). According to this definition of k_p, the weight change upon heating reflects only the weight gain of the ***oxygen*** reacted during the oxidation process. Upon cooling, spalling may take place, which will reflect the weight of the ***oxide*** segment lost (metal + oxygen). (Note that the term *weight* gain and loss are used according to a common convention, rather than *mass*).

The description of the spalling process requires a number of assumptions and a more detailed development. The present model is based on a simple spalling arrangement. It is assumed that a constant area fraction, F_A, will spall to the bare metal surface each cycle. Thus the sample can be viewed to be divided up into n_o equivalent segments, where $n_o = 1/F_A$, and each of these segments will have its own individual oxide growth and spallation history. These segments, with fractional area (F_A) and the equivalent of one time unit $\sqrt{(k_p \Delta t)}$ thick, will be the basic cells in constructing the model.

2.1. Primary spallation sequence

In Figure 1, a schematic cross-section of the oxidized surface is shown for the case where the area spall fraction $F_A = 0.1$ and thus $n_o = 10$ segments. The growth and spalling sequence of each i^{th} segment is presented for the first 5 cycles. For the sake of simplicity, the height of each oxide segment is represented here only by its corresponding amount of time elapsed. After one cycle, the entire surface has grown a scale according to equation 1 (above the zero-growth line) and one segment equivalent to one time unit thick has spalled (below the line). After two cycles, the still intact surface scale (for i = 3-10) has grown to a thickness corresponding to $\sqrt{(k_p 2\Delta t)}$. The first segment (i=1) has re-grown to $\sqrt{(k_p \Delta t)}$, and the second segment (i =2), having grown $\sqrt{(k_p 2\Delta t)}$, has now spalled. In these figures, sequential spalled segments are shown as adjacent segments for visual simplicity, but this is not required by the mathematics or in practice. This continuing sequence is outlined here for up to five cycles (j=5). Implicit in this progression is that the next segment to spall is **always** the thickest segment (or as thick as any other equivalent segments). There is no critical thickness at which spallation begins, however its effects are felt progressively as the scale thickens.

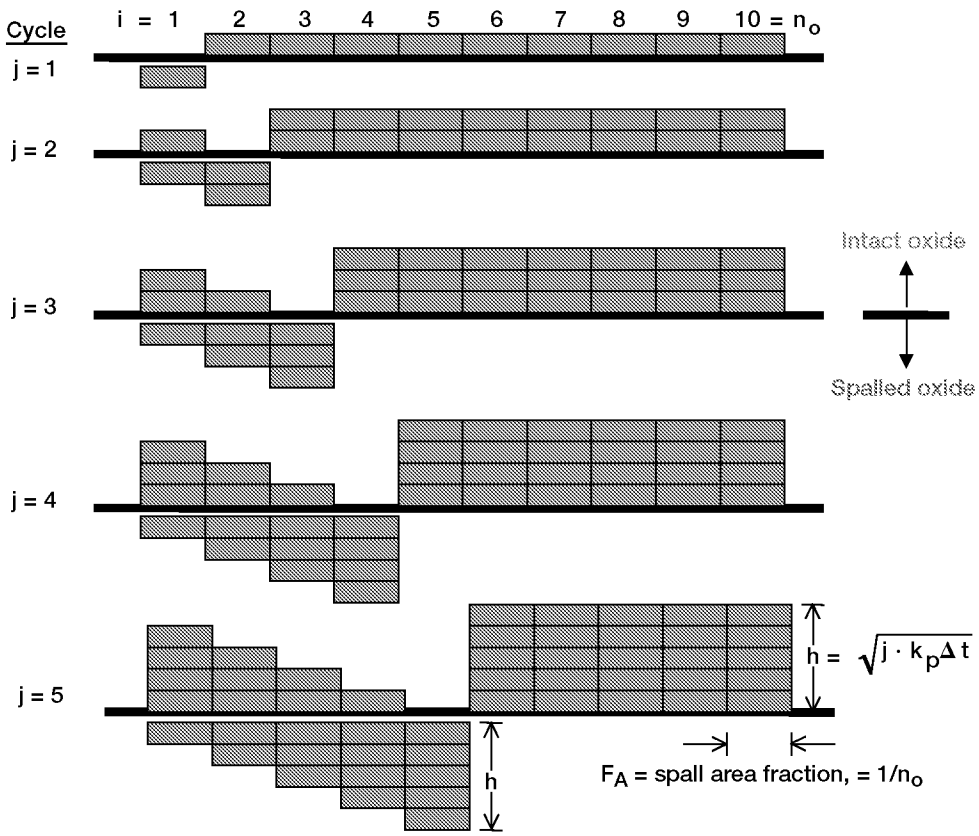

Figure 1.—Schematic cross-section of intact and spalled oxide segments (above and below the line) for the first five cycles of oxide growth and spallation. Case A, $j < n_o$. Each block corresponds to a basic unit F_A in area and $k_p\Delta t$ in height (weight).

In general, the weight **gain** (segment height) of oxide remaining in the intact segments is proportional to:

$$\Delta W / A = f(\sqrt{j \cdot k_p \Delta t}), \qquad [2]$$

for the relative area of the intact oxide region, $(n_o - j)\cdot F_A$. Here the weight gain reflects only the amount of oxygen in the segments, implicit in the definition of k_p.

However, the amount of weight **loss** due to spallation must take into account the weight of metal in the oxide. The weight of oxide relative to that of oxygen is given by a stoichiometric constant, S_c, defined as the molecular weight ratio of oxide to oxygen in any given oxide, e.g., Al_2O_3, Cr_2O_3, NiO, etc. Thus the oxide weight is obtained by multiplying the corresponding oxygen weight by S_c, and the amount of metal in a given segment is obtained by multiplying by $(S_c - 1)$.

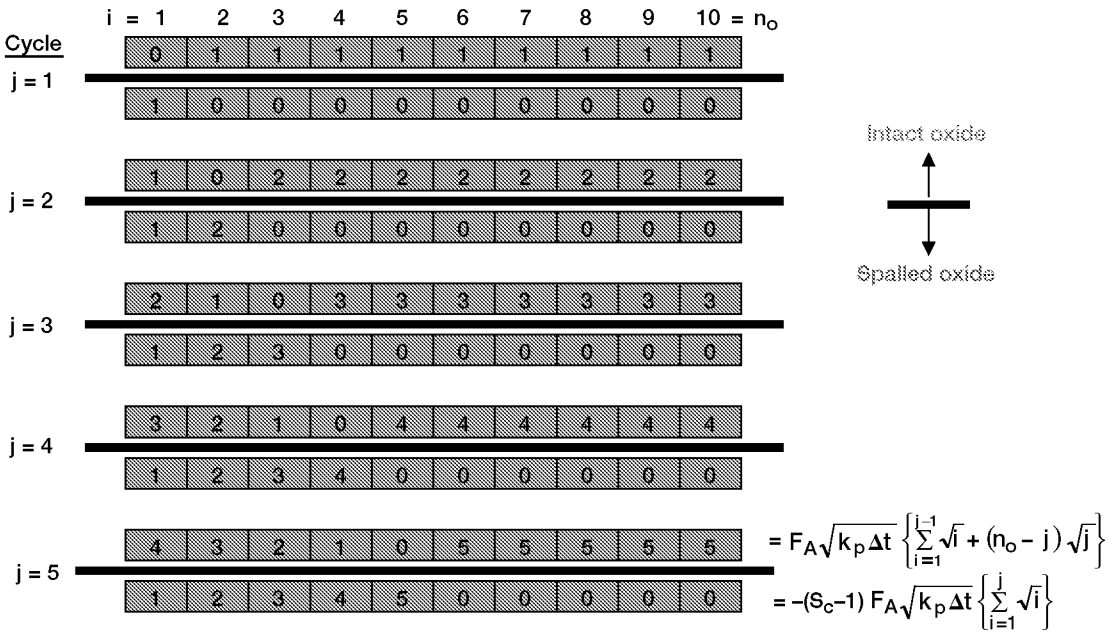

Figure 2.—Shorthand notation describing the intact and spalled segments for the first five cycles of oxide growth and spallation. Case A, $j < n_o$. Each block is labeled as to the number of cycle duration time units of height (weight).

A simplifying notation for this spalling sequence is shown in figure 2. Here the time unit of scale growth is labeled on each intact (green) segment above the zero-growth line or spalled (blue) area segment below the line. Thus it is seen that the weight gain of the left-most segments that have spalled once and re-grown new oxide is given by:

$$F_A \sum_{i=1}^{j-1} \sqrt{i \cdot k_p \Delta t} \qquad [3]$$

The weight gain of all the original intact right-most segments is given by:

$$(n_o - j)\, F_A \sqrt{j \cdot k_p \Delta t} \qquad [4]$$

Finally, the weight change due to just the metal lost in the spalled segments is given by:

$$-(S_C - 1)\, F_A \left\{ \sum_{i=1}^{j} \sqrt{i \cdot k_p \Delta t} \right\} \qquad [5]$$

The same sequence of growth and spallation can be envisioned to occur here for up to 10 cycles, ($j \le n_o$, case A), at which time the entire surface would have spalled just one time, and the number of cycles, j, is just equal to the number of segments, n_o.

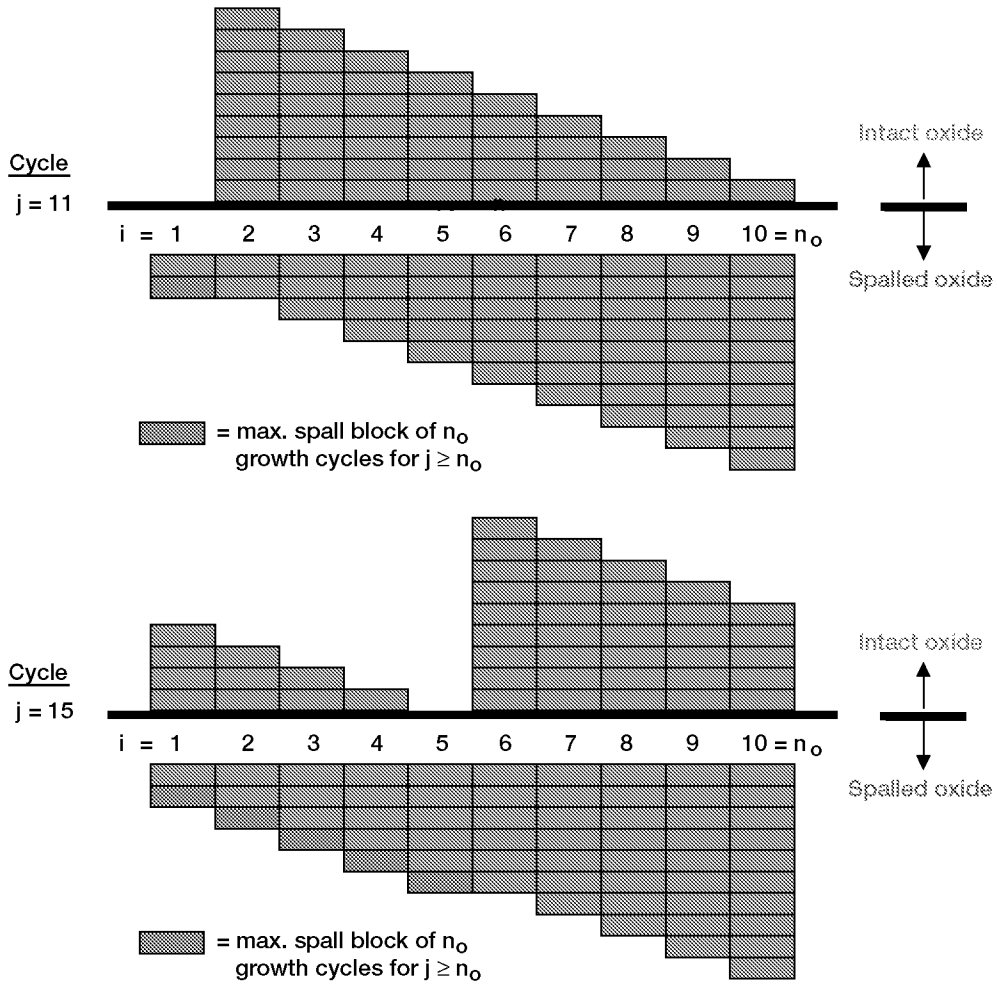

Figure 3.—Schematic cross-section of intact and spalled oxide segments (above and below the line) for the first 11 and 15 cycles of oxide growth and spallation. Case B, $j > n_o$. Each block corresponds to a basic unit F_A in area and $k_p\Delta t$ in height (weight).

Secondary and subsequent spallation sequences. For $j \geq n_o$, continued spallation produces a modification in the sequence. At j = 11, the first segment is now the thickest segment (corresponding to 10 Δt) and is sequenced for its second spallation event, as shown in figure 3a. At j = 12, the second segment spalls, also 10 time units thick. All new spall segments are now this maximum of 10 units ($n_o \cdot \Delta t$) thick. Thus, for visual simplicity and convenience, these secondary spall segments are all shown as solid blocks, for a segment height equivalent to j =10 in eq. 5. The continued progression of this secondary spall sequence leads to the schematic for the case j =15, shown in figure 3b.

The simplifying notation for Case B, where $j \geq n_o$, is given in figure 4. As can be seen for these three general cases where $j > 10\ n_o$, $j > 20\ n_o$, and $j > 30\ n_o$, the total amount of retained scale remains the same, even though the thickness over each particular area segment changes progressively each cycle. The oxygen gain obtained from all the segments above the zero-growth line is thus given by the invariant quantity:

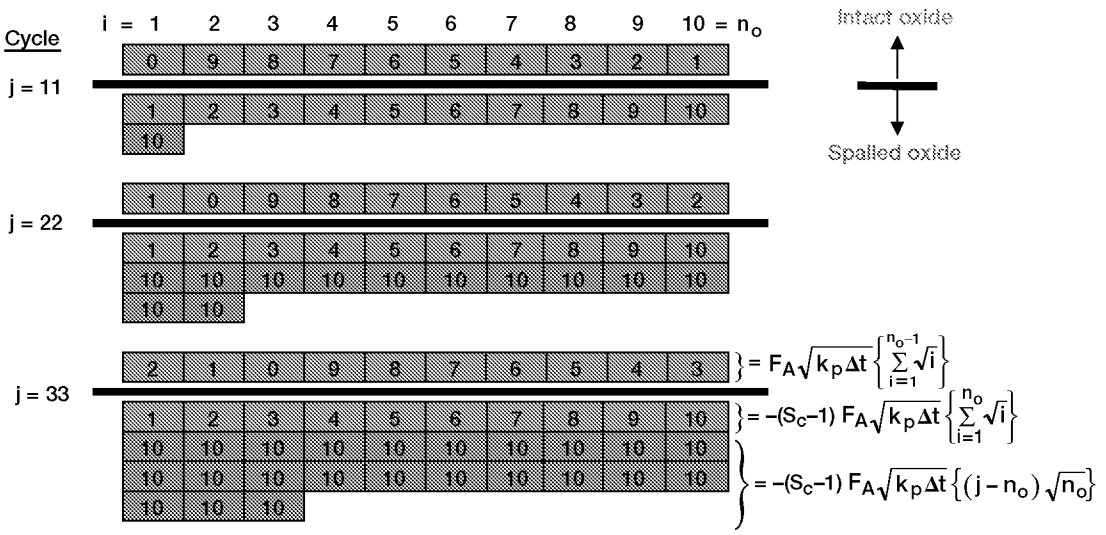

Figure 4.—Shorthand notation describing the intact and spalled segments for the 11, 22, and 33 cycles of oxide growth and spallation. Case B, $j > n_o$. Each block is labeled as to the number of cycle duration time units of height (weight).

$$F_A \sum_{i=1}^{n_o-1} \sqrt{i \cdot k_p \Delta t} \qquad [6]$$

Similarly, the metal loss due to the first series of spalled segments is invariant and is given by:

$$-(S_C - 1)\, F_A \left\{ \sum_{i=1}^{n_o} \sqrt{i \cdot k_p \Delta t} \right\}, \qquad [7]$$

while the series of the secondary spall segments produces the term:

$$-(S_C - 1) \cdot (j - n_o)\, F_A \sqrt{n_o \cdot k_p \Delta t} \qquad [8]$$

By combining all the appropriate oxygen gain and metal loss terms, plus some simplification of the summations, the following relationships are obtained describing cyclic oxidation net weight change according to this model:

For cycle number $j \leq n_o$ (Case A):

$$\left(\frac{\Delta W}{A}\right)_A = F_A \sqrt{k_p \Delta t} \left\{ (2 - S_c) \sum_{i=1}^{j} \sqrt{i} + (n_o - j - 1)\sqrt{j} \right\} \qquad [9]$$

And for cycle number $j \geq n_o$ (Case B):

$$\left(\frac{\Delta W}{A}\right)_B = F_A\sqrt{k_p \Delta t}\left\{(2-S_c)\sum_{i=1}^{n_o}\sqrt{i} + [(1-S_c)(j-n_o)-1]\sqrt{n_o}\right\} \qquad [10]$$

Consequently two relationships (A and B) are needed to construct a full, two-part model weight change curve, applied when the number of cycles, j, is less than or greater than the number of segments, n_o. An example of the net weight change curve is shown in figure 5 for the following input parameters: k_p=0.01 mg^2/cm^{4}hr, Δt =1.0 hr, F_A=0.001 (i.e., n_o=1000), and S_c=2.0, for j up to 2000 hr. The classic shape and the general characteristics of a cyclic oxidation weight change curve are produced. Here the response follows essentially parabolic growth initially, gradually degrades by spallation, and then produces a maximum in the weight change curve. A continual decrease in weight achieves negative values. When j = n_o, i.e., 1000, a steady state, linear rate of weight loss is obtained and continues indefinitely according to eq. [10], i.e., Case B of the present model. In reality, excessive solute depletion may eventually cause a critical composition to be reached that triggers a mechanism change.

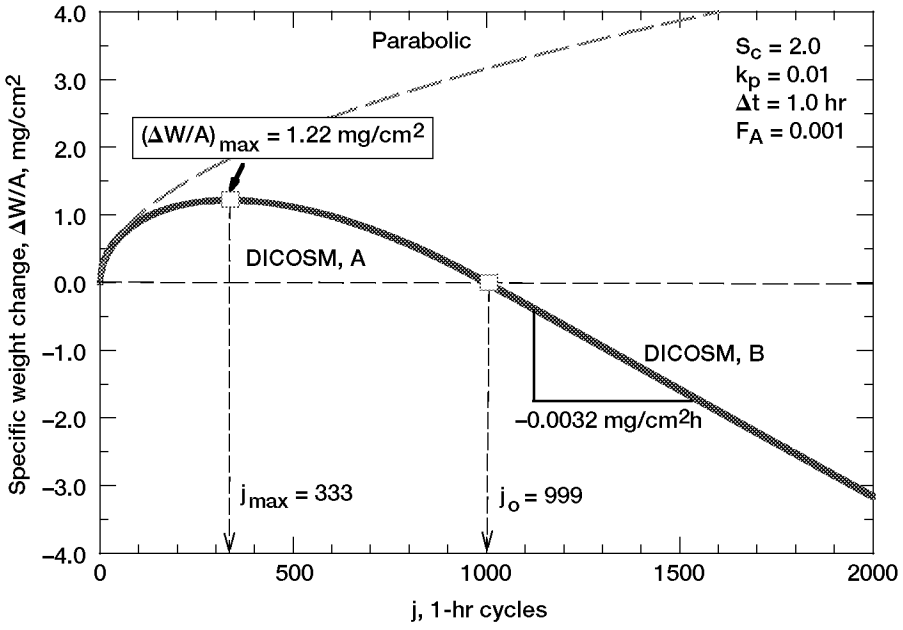

Figure 5.—DICOSM model curve of specific weight change vs cycle time for the parameters k_p = 0.01 mg^2/cm^4 hr, Δt = 1.0 hr, F_A = 0.001 (i.e., n_o = 1000), and S_c = 2.0.

TABLE 1.—LIST OF RELATIONSHIPS DESCRIBING OTHER PERTINENT QUANTITIES OBTAINED FROM DICOSM MODEL

Total amounts of oxygen and metal reacted:

$$\Sigma W_{oxy,A} = F_A\sqrt{k_p\Delta t}\left\{2\sum_{i=1}^{j}\sqrt{i} + (n_o - j - 1)\sqrt{j}\right\}$$

$$\Sigma W_{oxy,B} = F_A\sqrt{k_p\Delta t}\left\{2\sum_{i=1}^{n_o}\sqrt{i} + (j - n_o - 1)\sqrt{n_o}\right\}$$

$$\Sigma W_{met} = (S_c - 1)\,\Sigma W_{oxy}$$

Amount of scale retained before and after spallation:

$$W'_{r,A} = S_c F_A\sqrt{k_p\Delta t}\left\{\sum_{i=1}^{j}\sqrt{i} + (n_o - j)\sqrt{j}\right\}$$

$$W_{r,A} = S_c F_A\sqrt{k_p\Delta t}\left\{\sum_{i=1}^{j}\sqrt{i} + (n_o - j - 1)\sqrt{j}\right\}$$

$$W'_{r,B} = S_c F_A\sqrt{k_p\Delta t}\left\{\sum_{i=1}^{n_o}\sqrt{i}\right\}$$

$$W_{r,B} = S_c F_A\sqrt{k_p\Delta t}\left\{\sum_{i=1}^{n_o-1}\sqrt{i}\right\}$$

Total and fractional amounts of scale spalled:

$$\Sigma W_{s,A} = S_c F_A\sqrt{k_p\Delta t}\left\{\sum_{i=1}^{j}\sqrt{i}\right\}$$

$$\Sigma W_{s,B} = S_c F_A\sqrt{k_p\Delta t}\left\{\sum_{i=1}^{n_o}\sqrt{i} + (j - n_o)\sqrt{n_o}\right\}$$

$$F_{s,A} = \frac{\sqrt{j}}{\sum_{i=1}^{j}\sqrt{i} + (n_o - j)\sqrt{j}}$$

$$F_{s,B} = \frac{\sqrt{n_o}}{\sum_{i=1}^{n_o}\sqrt{i}}$$

2.2 Other outputs

While the weight change curve represents the most commonly measured value in practice, there are other terms that describe a number of significant aspects of the cyclic oxidation process. Some of these additional terms may also be easily obtained from the model described in figures 1-4, as listed below:

- Total amounts of oxygen and metal reacted
- Weight of retained oxide immediately before and after spallation
- Total amount of oxide spalled
- Fractional amount of oxide spalled per cycle

Relations for most of these terms are listed in table 1. Unfortunately, there are usually two equations for each, again depending on whether or not $j > n_o$. The total amount of oxygen reacted, $\Sigma W_{oxy,\,A}$, for Case A can be determined from inspection of figures 1 and 2 using the terms [3-5], but without the contribution of the metal stoichiometric factor (S_c-1). The same is true for Case B, using terms [6-8] along with figures 3 and 4. The metal reacted for both cases is simply the amount of oxygen reacted multiplied by (S_c-1).

The oxide retained after spalling, W_r, corresponds to the weight of oxygen in all the intact growth segments (above the line) multiplied by S_c. Thus for Case A, the segments described by the terms in [3, 4] apply, but must be multiplied by the stoichiometric factor, S_c. For Case B, the segments in term [6] applies. The oxide retained just before cooling (spalling), W_r', is obtained by adding the weight of the last spall segment to W_r.

The total amount of oxide spalled for Case A and B can be obtained from the terms [5] and [7, 8], respectively, which must account for all the segments below the line, multiplied by the stoichiometric factor, S_c. Finally, the fraction of oxide spalled on any given cycle is given by the weight of the current spall segment divided by that of the total amount of retained oxide just before spallation (cooldown), W_r'. That is, a spalled segment with a time unit of $j \cdot \Delta t$ or $n_o \cdot \Delta t$ should be divided by $W'_{r,A}$ or $W'_{r,B}$, respectively.

These other outputs are plotted in figure 6 for the same model conditions as those in figure 5. The oxygen and metal reacted follow similar trends as might be expected. However, in this special case where S_c=2, these quantities are identical because the metal component of the oxide, S_c-1, is exactly the same as the oxygen component, 1. The amount of retained oxide follows a gradual gain and becomes constant at $j = n_o$. The amount of oxide spalled follows a gradually increasing rate that becomes a constant rate at $j = n_o$. The fractional amount of oxide spalled, compared to the retained scale before cooling, also follows an increasing rate. But this parameter becomes a constant amount at $j = n_o$, equal to ~3/2 F_A, as will be derived in Part 2.

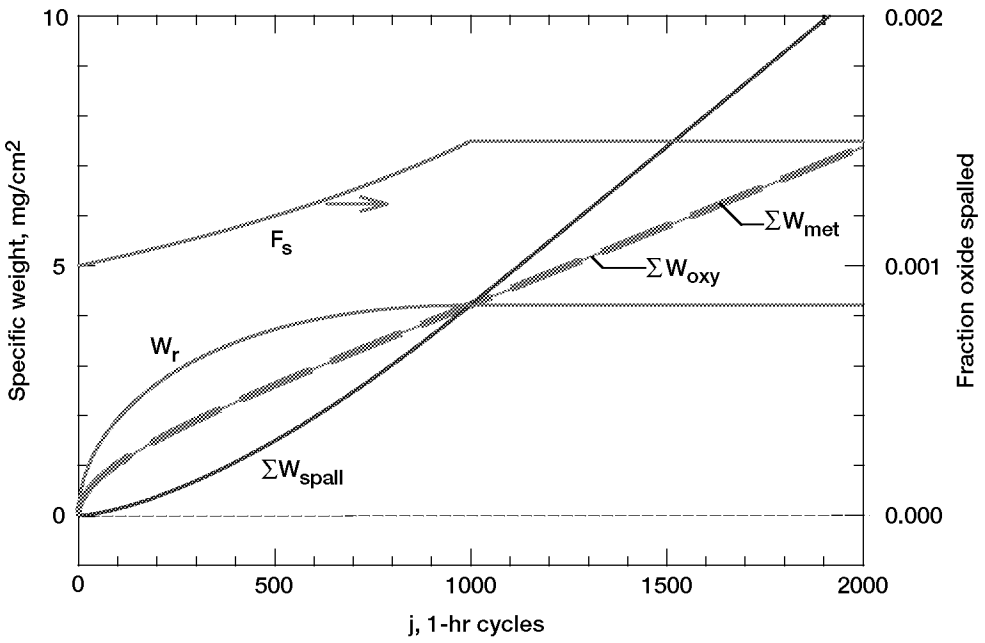

Figure 6.—Other DICOSM model outputs (total amount of oxygen and metal reacted, amount of retained scale and fraction of scale spalled, total amount of spalled scale.) vs cycle time for the parameters k_p = 0.01 mg^2/cm^4 hr, Δt = 1.0 hr, F_A = 0.001 (i.e., n_o = 1000), and S_c = 2.0.

3. Effects of Model Inputs

A number of characteristic trends in a classic weight change curve occur as the input parameters are varied. These trends are illustrated by the families of curves in figures 7-10 generated by increasing one input variable at a time, with the direction of the trend shown by dashed arrow. A common baseline curve is always presented for S_c = 2.0, k_p = 0.01 mg/cm^{2}hr, F_A = 0.001, and Δt = 1 hr. For figures 7-9, Δt is fixed at 1 hr per cycle, and the curves are identical whether the plots are against oxidation time or number of cycles. The range of parameters addressed by these curves were chosen to most graphically illustrate effects on the weight change curve in the region of ±5 mg/cm^2 and for the cycle (time) range of about 1000 hr. This would correspond to the behavior of many oxidation resistant materials operating at temperatures where appreciable, but not catastrophic, degradation is sustained.

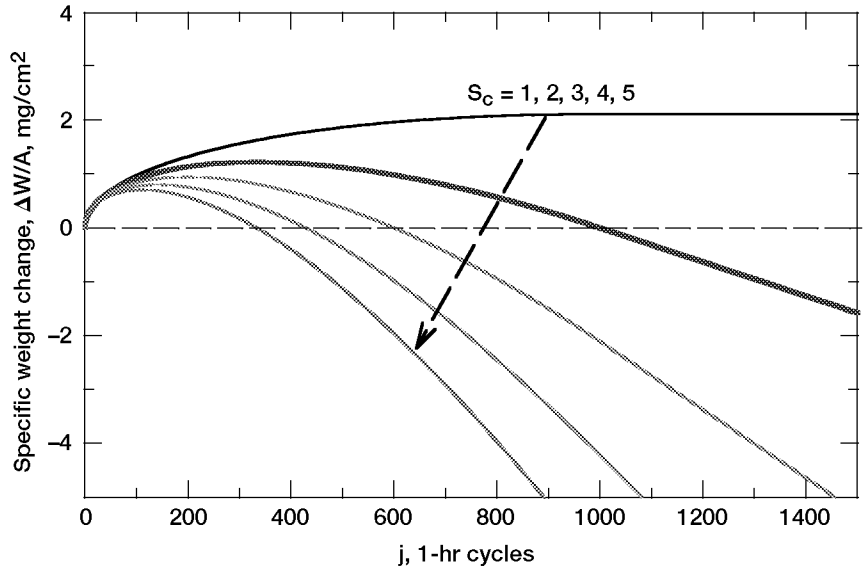

Figure 7.—The effect of the stoichimetric constant, S_c, on the family of DICOSM weight change curves. Baseline value of S_c = 2.0 shown as bold line. (k_p = 0.01 mg^2/cm^4 hr, Δt = 1.0 hr, F_A = 0.001).

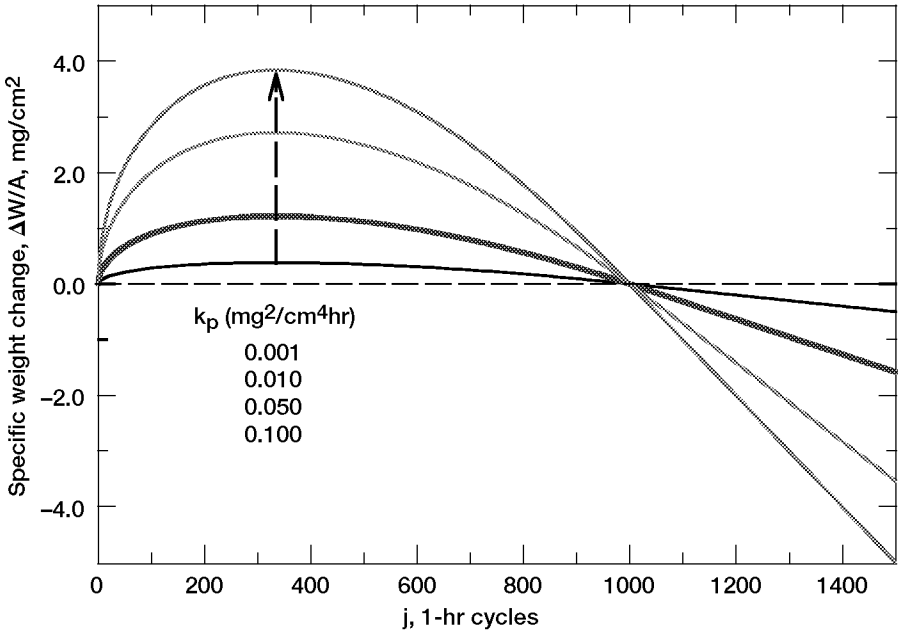

Figure 8.—The effect of the parabolic growth rate, k_p, on the family of DICOSM weight change curves. Baseline value of k_p = 0.01 mg^2/cm^4 hr shown as bold line. (S_c = 2.0, Δt = 1.0 hr, F_A = 0.001).

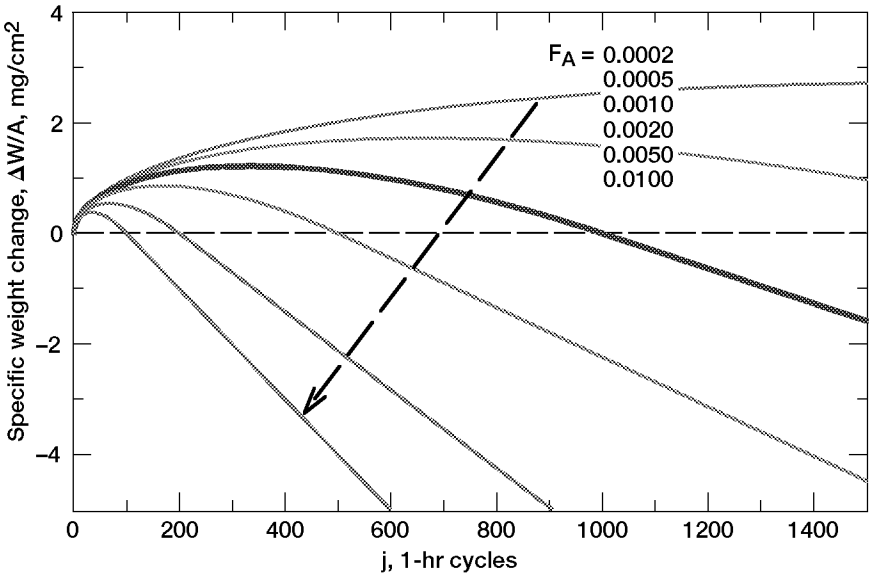

Figure 9.—The effect of spall area fracture, F_A, on the family of DICOSM weight change curves. Baseline value of F_A = 0.001 shown as bold line. (S_c = 2.0, k_p = 0.01 mg^2/cm^4, Δt = 1.0 hr).

The curves in figure 7 show the effect of increasing the stoichiometric constant from 1.0 to 5.0 on the net weight change. Most common oxides possess an S_c between 2 and 5, as listed in table 2 in order of increasing atomic number of the metal cation. Some widely observed oxides composed of two cations are also listed. Al_2O_3, for example, is relatively low at 2.1243. Very few oxides have lower S_c that might actually be produced on a high temperature alloy. Intermediate values are observed for NiO (4.6690) and the mixed spinel oxide $NiAl_2O_4$, (2.7603). Very high values are possible for the heaviest cations, such as ThO_2 (8.2515), or for cation-rich stoichiometry, such as Cu_2O (8.9435).

The value of S_c=1, corresponding to no cation weight in the scale, does not represent a real system. It is shown here to indicate the upper bound of behavior for oxides with lower metal contents. In that extreme, no maximum is produced, but a constant positive weight change is maintained at long times. The trend with increasing metal content in the oxide is a downward compression toward the origin and: (a) a progressive decrease in the number of cycles to maximum and zero weight change, (b) a decrease in the maximum in weight change, and (c) an increase in the final rate of weight loss. These effects are rather strong considering that S_c was only varied by a factor of 5.

The effect of increasing the growth constant, k_p, two orders of magnitude from 0.001 to 0.1 is shown in figure 8. The curves show a vertical amplification of both the weight gains and losses, but without a lateral shift on the cycle time axis: the maximum in the weight gain increases, as does the final linear rate of weight loss. However the number of cycles to maximum and zero weight change do not change.

TABLE 2.—STOICHIOMETRIC CONSTANT, S_C, (WEIGHT OF OXIDE TO OXYGEN) FOR MANY COMMON OXIDES

ROW	Atomic number	OXIDE	S_c
2	3	Li_2O	1.8675
	4	BeO	1.5633
	5	B_2O_3	1.4500
3	11	Na_2O	3.8738
	12	MgO	2.5191
	13	Al_2O_3	2.1243
	14	SiO_2	1.8777
4	22	TiO_2	2.4959
	23	V_2O_5	2.2736
	24	Cr_2O_3	3.1666
	25	Mn_2O_5	2.3735
	25	Mn_2O_3	3.2892
	26	Fe_2O_3	3.3270
	26	Fe_3O_4	3.6178
	26	FeO	4.4904
	27	CoO	4.6835
	28	NiO	4.6690
	29	CuO	4.9718
	29	Cu_2O	8.9435
5	40	ZrO_2	3.8509
	41	Nb_2O_5	3.3227
	42	MoO_3	2.9988
6	72	HfO_2	6.5780
	73	Ta_2O_5	5.5239
	74	WO_3	4.8301
7	90	ThO_2	8.2515
Mixed	13,14	$Si_2Al_6O_{13}$	2.0484
	13,22	$TiAl_2O_5$	2.2729
	13,39	$AlYO_3$	3.4144
	13,28	$NiAl_2O_4$	2.7603
	24,28	$NiCr_2O_4$	3.5421
	22,28	$NiTiO_3$	3.2201
	28,73	$NiTa_2O_6$	5.3813
	24,41	$CrNbO_4$	3.2642
	24,73	$CrTaO_4$	4.6339
	28,74	$NiWO_3$	4.7897

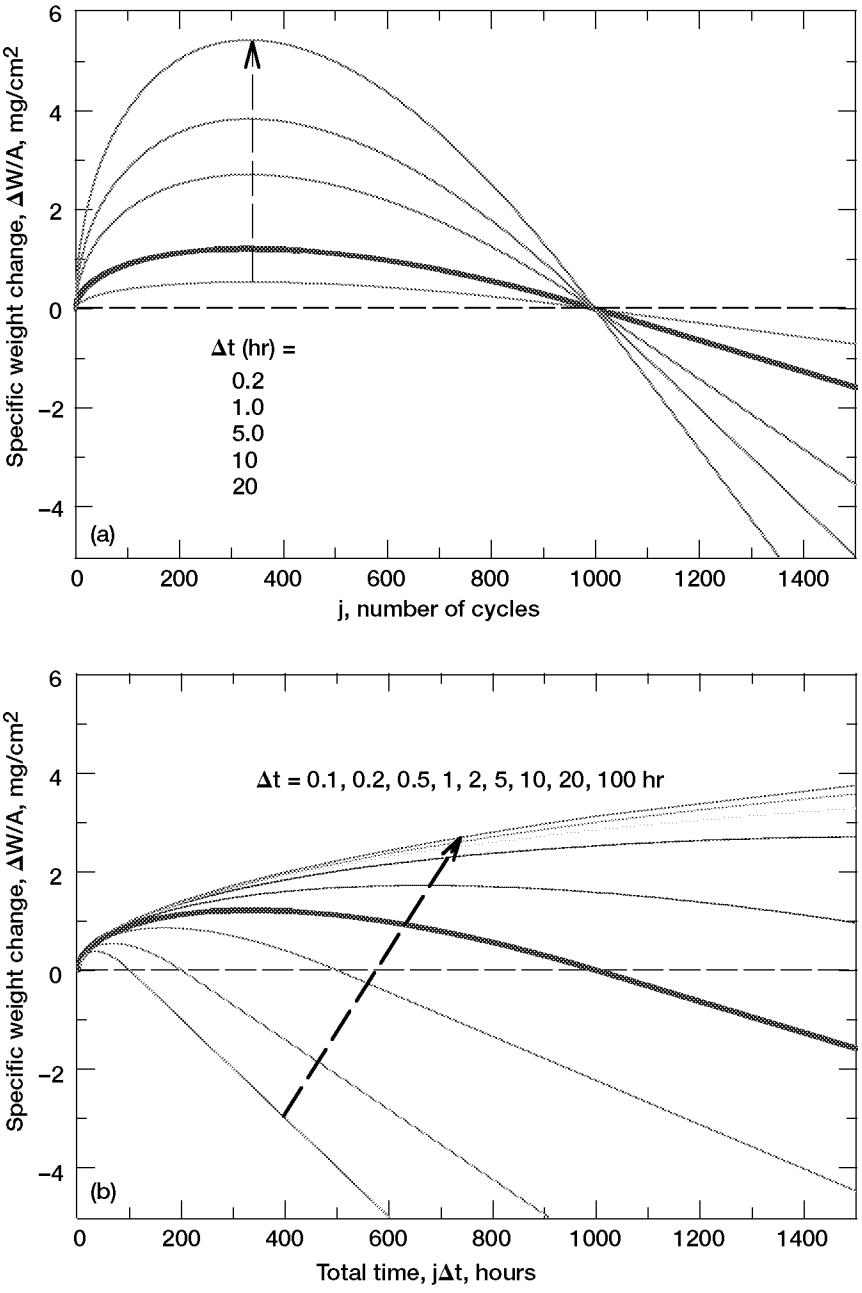

Figure 10.—The effect of cycle duration Δt, on the family of DICOSM weight change curves. Baseline value of Δt = 1.0 hr hr shown as bold line. (S_c = 2.0, k_p = 0.01 mg^2/cm^4h, F_A = 0.001). (a) Compared on the basis of the number of cycles, j. (b) compared on the basis of the total oxidation time, j·Δt.

Figure 9 presents the trend in weight change curves with increasing the spalling (area) fraction, F_A, which is similar to that observed for S_c. A compression toward the origin and downward is again apparent, but with not as strong a dependence. An upper bound to the curves is defined by $F_A = 0$, which is simply the continuously rising parabolic growth curve, with no spalling. As the values of F_A approach unity, the apparent maximum in weight gain is essentially eliminated, and the linear rate of weight loss starts immediately.

The effect of increasing cycle duration from 0.1 to 20 hr per cycle is shown in figure 10a. The trend in the family of curves shows a vertical amplification in the maximum weight change and linear rate of weight loss, with no lateral shift in the number of cycles to reach maximum or zero weight change. It causes exactly the same effect as increasing k_p, as might be expected from examining equations [9,10]. However it must be noted that the abscissa is specifically the number of cycles here, whereas it had previously been equivalent to both the number of cycles or total time in figures 7-9 because there Δt had always been fixed at 1 hr.

When the data of figure 10a is re-plotted against total oxidation time, figure 10b, the family is much the same as that for F_A, but trending in the reverse direction (upward and away from the origin). That is, the time to reach maximum and zero weight change and the maximum weight level achieved all increase with cycle duration.. Ultimately the pure parabolic growth curve is approached for very long cycle durations. Thus on a per cycle basis, longer cycle durations would produce more severe degradation, but on a per hour basis they would be less severe.

4. Comparison to Other Models

Some perspective on the applicability of this spalling model can be assessed by comparing it to other more established models. The earliest version of the interfacial spalling model also presumed that a constant area fraction spalled to bare metal each cycle [2]. However, instead of biasing the spallation event to only the thickest oxide segment, this model assumed that each new segment also spalls the same area fraction. This leads to an extremely complex scale structure with 2^J total segments and correspondingly complex iterative calculations. However, for most systems of interest, the area spall fraction is not much greater than 0.01 (1 percent of the area spalls each cycle). For these cases, most of the weight change is controlled by the 99 percent of the original area that remained intact and the small percent that spalls from this segment each successive cycle. In this regard, it is very similar to the DICOSM model, and this will become evident in the discussion on the descriptive parameters in Part II.

The models described in COSP (Cyclic Oxidation Spalling Program) are more versatile and completely developed [3-5]. This program may simulate spallation from the outer surface as a uniform layer over the entire surface or as interfacial spallation of discrete segments. The latter method involves a randomized probability (Monte Carlo) technique to determine whether a given segment spalls or remains intact (bimodal) on any given

cycle. Both methods are governed by one basic formula defining the weight fraction of spalled oxide on a given cycle:

$$F_s = Q_o W_r'^{\alpha} \qquad [11]$$

where F_s is the weight fraction of scale spalled, Q_o is a spall constant, W_r' is the weight of intact scale prior to cooling, and the exponent 'α' is a constant, usually taken to be 1.0.

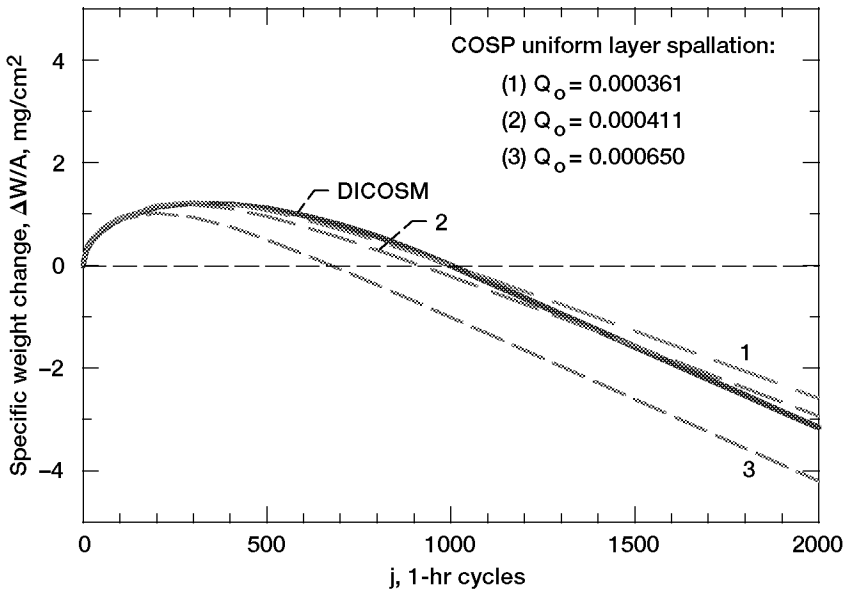

Figure 11.—Matching attempts of three uniform spalling layer COSP model curves to baseline DICOSM curve on the basis of (1) j_o, (2) F_s, and (3) T.S., see Table 3. (S_c = 2.0, k_p = 0.01 mg^2/cm^4, Δt = 1.0 hr).

The baseline DICOSM curve is shown as a bold curve in figure 11 along with three corresponding COSP curves for uniform layer spallation corresponding to the same stoichiometric constant and k_p. COSP curve #1 was generated so that the cycles to zero weight change matched those of the baseline DICOSM case. Reasonable agreement occurs up to j_o, but some deviation accrues for the steady state linear loss portion. The second COSP curve was produced by matching the spall fraction, F_s, and shows better agreement in the steady state weight loss region, but less agreement in the initial portion, $j < j_o$. The COSP curve #3 was produced with the same final slope as the DICOSM plot, but is considerably more offset compared with the other two COSP curves.

These results are summarized in table 3, listing the various input parameters and summarizing the key descriptive output parameters. (The characteristics that were matched to the DICOSM model are highlighted). Here it can be seen quantitatively that there are minor deviations in the other outputs for each trial case. Also shown are the results for a COSP model (#1b) where the Q_o parameter was matched to that defined by the steady state portion of the DICOSM plot and is very close to the COSP (#1a) model. Thus it is seen that all four attempts to match the constant spall area fraction model

(DICOSM) with the uniform layer spalling model (COSP) produced similar, but not entirely congruent, curves.

TABLE 3.—A COMPARISON OF DICOSM MODEL RESULTS WITH COSP UNIFORM OUTER LAYER AND BIMODAL INTERFACIAL (MONTE CARLO) SPALLING MODES

(Boldface indicates intended matching of a parameter with DICOSM model.
N.A. indicates Not Appropriate for calculating spall fraction because of random variations.)

	DICOSM fixed	COSP-1a uniform	COSP-1b uniform	COSP-2 uniform	COSP-3 uniform	COSP-4 bimodal	COSP-5 bimodal	COSP-6 bimodal
				(A) inputs				
S_c	2.0	2.0	2.0	2.0	2.0	2.0	2.0	2.0
k_p	0.01	0.01	0.01	0.01	0.01	0.01	0.01	0.01
Δt	1.0	1.0	1.0	1.0	1.0	1.0	1.0	1.0
F_A	0.001	------	------	------	------	------	------	------
α		1.0	1.0	1.0	1.0	1.0	0.5	0.0
Q_o	(0.000355)	0.000361	**0.000355**	0.000411	0.000650	0.000343	0.000675	0.001250
N_{seg}	1000	------	------	------	------	1000	1000	1000
				(B) outputs				
j_o	**999**	**999.0**	1009.3	915.6	674.0	973.4	992.7	1004.9
TS	**0.0032**	0.0026	0.0026	0.0027	**0.0032**	**0.0034**	**0.0033**	**0.0032**
F_s	**0.00150**	0.00138	0.00136	**0.00150**	0.00204	N.A.	N.A.	N.A.
ΣW_{met}	7.3786	6.3993	6.3783	6.5838	7.3333	7.7707	7.7372	7.5297

This matching exercise was repeated for the bimodal interfacial (Monte Carlo, $R_{spall} = 1.0$) spalling format within COSP as well, figure 12. In this figure the two COSP models (#4, 5) were iteratively adjusted to give the best overall visual fit. Model #4 used a Q_o value not too different from those used in the uniform spalling cases. It is seen to produce a reasonably close value of j_o and the final (terminal) slope, TS. The fluctuation of the data points is produced by the randomized nature of the Monte Carlo spalling process. The other model attempted (#5), using the exponent, α, of 0.5, produced a somewhat better overall match with similar output parameters. Finally, the case (#6) where the spall weight fraction was always constant, i.e., $\alpha = 0.0$, as in the steady state portion of the DICOSM model, matched the DICOSM model outputs best of all, table 3.

Thus the DICOSM model appears to reproduce the behavior of the bimodal COSP model, but without the element of variability introduced by the Monte Carlo method of determining whether a given element spalls on a given cycle. DICOSM does not, however, accurately reproduce the uniform layer COSP model curves, although the basic shapes are similar. A more mathematical description and comparison of the models can be made if the key descriptive factors can be summarized in algebraic expressions. By means of an approximation to the summation series in eq.'s. [9,10], the weight change curve, the model outputs, and key descriptive parameters will be expressed by simple mathematical relationships in Part II. This will allow the complete definition of cyclic

oxidation response as a function of all the model inputs without the need for a programmed, iterative (computer) calculation. These expressions led to a more generalized perspective, enabling the concept of normalizing any cyclic oxidation model curve or actual data into a universal cyclic oxidation curve.

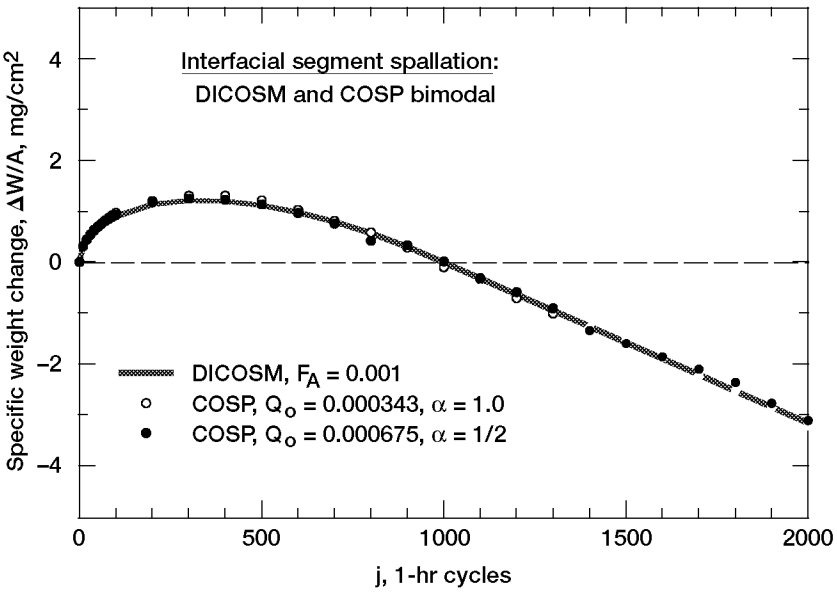

Figure 12.—Matching attempts of two bimodal (interfacial) Monte Carlo spalling segment COSP cases (number 4 and 5) to baseline DICOSM curve on the basis of terminal slope, T.S., see Table 3. (S_c = 2.0, k_p = 0.01 mg^2/cm^4, Δt = 1.0 hr).

5. Summary

A model for cyclic oxidation scale growth and spallation has been constructed. It is predicated on parabolic scale growth and a constant area fraction of spallation. Spallation is always assumed to be interfacial and is biased to the thickest segment of intact oxide (deterministic). The weight change behavior can be described in-full by a two-part equation, depending on whether the number of cycles in the model, j, is greater than or less than the number of segments. Model cyclic oxidation curves exhibit all the typical characteristics of other models and experimental data: a maximum in weight gain followed by a decrease to zero weight gain and an eventual linear (steady state) rate of weight loss. The effects of stoichiometric constant, parabolic growth rate, spall parameter, and cycle duration all produce regular trends in the response, with reasonable similarities to previous models. An inherent asset of the present model is its mathematical simplicity and its deterministic criterion for spallation.

References

1. Barrett, C.A., A Statistical Analysis of Elevated Temperature Gravimetric Cyclic Oxidation Data of 36 Ni- and Co-Base Superalloys Based on an Oxidation Attack Parameter. Washington, DC. NASA TM–105934, 1992.

2. Smialek J.L., Metall. Trans. 1978, 9A: 309–320.

3. Lowell, C.E., Smialek, J.L., Barrett, C.A., Cyclic Oxidation of Superalloys. In R.A. Rapp, ed., High Temperature Corrosion. Houston, TX. NACE 6, 1983. pp 219–226.

4. Lowell, C.E., Barrett, C.A., Palmer, R.W., Auping, J.V., Probst, H.B., Oxid. Met., 1991, 36: 81–112.

5. Smialek, J.L., Auping, J.V., Oxid. Met. 2002, 57: 559–581.

6. Nesbitt, J.A., In Romig, A.D., Dayanada, M.A., eds., Diffusion Analysis and Applications. Warrendale, PA. TMS–AIME, 1989. pp 307–324.

7. Smialek, J.L., Nesbitt, J.A., Barrett, C.A., Lowell, C.E., Cyclic Oxidation Testing and Modelling: a NASA Lewis Perspective. In Schütze, M., Quadakkers, W.J., eds., Cyclic Oxidation of High Temperature Materials. European Federation of Corrosion. London, UK. Institute of Materials; 1999. pp 148–168.

8. Schütze, M., Quadakkers, W.J., eds., Cyclic Oxidation of High Temperature Materials. European Federation of Corrosion. London, UK. Institute of Materials, 1999.

9. Evans, H.E., Int. Met. Rev. 1995, 40: 1

10. Tolpygo, V.K., Dryden, J.R., Clarke, D.R., Acta Mater. 1998, 46: 927–937.

11. Wang, J-S, Evans, A.G., Acta Mater. 1998, 46: 4993–5005.

12. Tolpygo, V.K., Clarke, D.R., Mater. Sci. Eng., 2000, A278: 142–150 and 151–161.

13. Chan, K.S., Metall. and Mater. Trans. 1997, 28A: 411–422.

14. Moon, C.O., Lee, S.B., Oxid. Met. 1993, 39: 1–13.

15. Haynes, J.A., More, K.L., Pint, B.A., Wright, I.G., Cooley, K., Zhang, Y., Mater. Sci. Forum. 2001, 369–372; 679–686.

16. Tolpygo, V.K., Clarke, D.R., Murphy, K.S., Metall. Mat. Trans. 2001, 32A: 1467–1478.

17. Smialek, J.L., Pint, B.A., Mater. Sci. Forum. 2001, 369–372: 459–466.

Appendix: Glossary of Terms

i	oxide segment index
j	number of oxidation cycles
j_{max}	cycle number to reach maximum weight gain
j_o	cycle number to reach zero weight change
$(\Delta W/A)$	specific weight change, (mg/cm^2)
$(\Delta W/A)_{max}$	maximum in cyclic oxidation weight change curve, (mg/cm^2)
n_o	number of oxide segments
F_a	spall area fraction constant = $1/n_o$
k_p	parabolic growth rate, (mg^2/cm^4h)
Δt	heating cycle duration, (h)
S_c	stoichiometric constant, weight fraction of oxide/oxygen
W_r	weight of oxide retained after cooldown, (mg/cm^2)
W_r'	weight of oxide retained before cooldown, (mg/cm^2)
ΣW_{met}	cumulative amount of metal consumed, (mg/cm^2)
ΣW_{oxy}	cumulative amount of oxygen consumed, (mg/cm^2)
ΣW_{spall}	cumulative amount of oxide spalled, (mg/cm^2)
F_s	weight fraction of oxide spalled
TS	terminal slope of weight change curve, (mg/cm^2h)

REPORT DOCUMENTATION PAGE

Form Approved
OMB No. 0704-0188

1. AGENCY USE ONLY (*Leave blank*)	2. REPORT DATE	3. REPORT TYPE AND DATES COVERED
	December 2002	Technical Memorandum

4. TITLE AND SUBTITLE

A Deterministic Interfacial Cyclic Oxidation Spalling Model:
Part 1.—Model Development and Parametric Response

5. FUNDING NUMBERS

WBS–22–708–73–05

6. AUTHOR(S)

James L. Smialek

7. PERFORMING ORGANIZATION NAME(S) AND ADDRESS(ES)

National Aeronautics and Space Administration
John H. Glenn Research Center at Lewis Field
Cleveland, Ohio 44135–3191

8. PERFORMING ORGANIZATION REPORT NUMBER

E–13596–1

9. SPONSORING/MONITORING AGENCY NAME(S) AND ADDRESS(ES)

National Aeronautics and Space Administration
Washington, DC 20546–0001

10. SPONSORING/MONITORING AGENCY REPORT NUMBER

NASA TM—2002-211906-PART1

11. SUPPLEMENTARY NOTES

Responsible person, James L. Smialek, organization code 5160, 216–433–5500.

12a. DISTRIBUTION/AVAILABILITY STATEMENT

Unclassified - Unlimited
Subject Category: 26 Distribution: Nonstandard

Available electronically at http://gltrs.grc.nasa.gov

This publication is available from the NASA Center for AeroSpace Information, 301–621–0390.

12b. DISTRIBUTION CODE

13. ABSTRACT ***(Maximum 200 words)***

An equation has been developed to model the iterative scale growth and spalling process that occurs during cyclic oxidation of high temperature materials. Parabolic scale growth and spalling of a constant surface area fraction have been assumed. Interfacial spallation of the only the thickest segments was also postulated. This simplicity allowed for representation by a simple deterministic summation series. Inputs are the parabolic growth rate constant, the spall area fraction, oxide stoichiometry, and cycle duration. Outputs include the net weight change behavior, as well as the total amount of oxygen and metal consumed, the total amount of oxide spalled, and the mass fraction of oxide spalled. The outputs all follow typical well-behaved trends with the inputs and are in good agreement with previous interfacial models.

14. SUBJECT TERMS

High temperature; Oxidation; Metals; Spalling; Computer programs; Thermal cycling; Modeling; Kinetics; Nickel alloys

15. NUMBER OF PAGES

28

16. PRICE CODE

17. SECURITY CLASSIFICATION OF REPORT	18. SECURITY CLASSIFICATION OF THIS PAGE	19. SECURITY CLASSIFICATION OF ABSTRACT	20. LIMITATION OF ABSTRACT
Unclassified	Unclassified	Unclassified	